Chapter 8

Novel Pressure-Induced Molecular Transformations Probed by *In Situ* Vibrational Spectroscopy

Yang Song

Additional information is available at the end of the chapter

http://dx.doi.org/10.5772/64617

Abstract

Pressure-induced structural change in molecular systems has demonstrated strong promises to access previously unexplored, novel structures and new properties in molecular materials with practical applications. The *in situ* structural characterization is of fundamental importance to understand the exotic structures and the possible transformation mechanisms. Among all the spectroscopic probes, vibrational spectroscopy that include Raman and Fourier-transform infrared (FTIR) spectroscopy and microscopy allow for highly efficient, sensitive and qualitative characterization of pressure-induced new structures and transformation processes *in situ*. Supported by state-of-the-art, highly customized spectroscopic systems in-house and at synchrotron facilities, molecular structures and materials properties can be probed in a broad pressure-temperature range with very high spectral and spatial resolutions. Complementary to each other, Raman and IR spectroscopy provide valuable information in molecular structures, nature of bonding, lattice dynamics as well as intermolecular interactions. In this chapter, a comprehensive and critical review of examples of pressure-induced molecular transformations in a wide variety of molecules and materials probed by vibrational spectroscopy is provided. The purpose of this chapter is to give readers the most recent advances in high-pressure chemistry and materials research by demonstrating the power of vibrational spectroscopy as a highly effective *in situ* structural characterization tool.

Keywords: high pressure, diamond anvil cells, Raman spectroscopy, FTIR spectroscopy, conformation, hydrogen bonding, phase transitions, guest-host interactions

1. Introduction

As one of three principal thermodynamic variables, pressure (P) plays an important role to alter the interatomic distances and thus the nature of intermolecular interactions, chemical bonding, molecular configurations, crystal structures and stability of materials. Extreme pressure can even induce transformations involving the strongest chemical interactions that exceed 10 eV (965 kJ mol^{-1}) such that chemical bonds and even the well-known properties of atoms and molecules can be completely changed. As a result, investigation of pressure-induced structural transformations and formation of novel functional materials has become a vibrant frontier in chemistry and materials science [1]. On one hand, major advances in high-pressure techniques such as diamond anvil cell have allowed the study of molecules and materials in an unprecedented pressure-temperature (P-T) range. On the other hand, the compatible micro-spectroscopic probes have made possible the characterization of structures and transformational processes *in situ* with great spectral and spatial resolution. The recent advances in high-pressure science and technology and their applications in materials research have been provided in several excellent review articles [2–8].

Among all the available *in situ* structural characterization probes for materials under extreme conditions, in particular, vibrational spectroscopy that include Raman and Infrared (IR) spectroscopy has demonstrated strong sensitivity and accuracy as well as efficiency in monitoring the pressure-induced transformations. Raman and IR spectroscopy, complementary to each other, provide valuable information on molecular structures, nature of bonding, lattice dynamics as well as intermolecular interactions. In this chapter, a comprehensive and critical review of examples of pressure-induced molecular transformations in a wide variety of molecules and materials probed by vibrational spectroscopy is given. The examples include (1) conformational change; (2) pressure-mediated hydrogen bonding; (3) phase and structural transitions; (4) pressure-induced chemical reactions; and (5) porous materials and guest-host interactions. Through these examples, the readers are provided the most recent advances in high-pressure chemistry and materials research by demonstrating the power of vibrational spectroscopy as an effective tool for structural characterizations for materials under extreme conditions.

2. Experimental methods

2.1. The diamond anvil cell

The recent advances in high-pressure technology have enabled the generation of extreme conditions in a broad P-T range with great controllability and accuracy. In particular, diamond anvil cell (DAC) is a fundamental apparatus to achieve static high pressures. Diamonds are known as the hardest material in nature and thus suitable as anvils to generate very high pressure. Moreover, diamonds are transparent to a wide spectral range of electromagnetic radiation from far-IR to hard X-ray. As a result, various analytical probes, including optical spectroscopy, synchrotron and neutron sources, have enabled structural characterization of

http://dx.doi.org/10.5772/64617

material under extreme P-T conditions with unprecedented spatial, temporal and spectral resolutions.

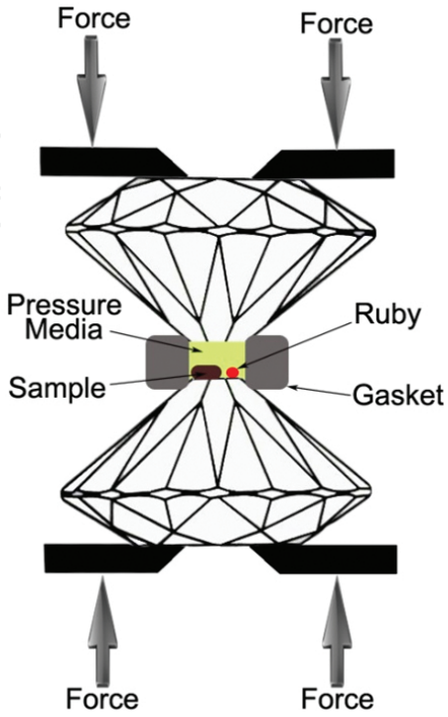

Figure 1. Schematic diagram of a diamond anvil cell.

Figure 1 shows a typical DAC apparatus where two brilliant cut diamonds are used as anvils to exert static pressure up to several million atmospheres (or several hundred GPa) with only moderate force. A metal gasket with a hole drilled at the center serves as the sample chamber. Most of the time the sample to be studied is loaded together with pressure-transmitting medium (PTM) to enhance the hydrostaticity, and a ruby chip which is used for pressure calibration. The extreme pressures can be accurately determined by monitoring ruby fluorescence lines using the following relationship [9]:

$$P = \frac{1904}{B}\left[\left(1+\frac{\Delta\lambda}{694.24}\right)^{B}-1\right] \quad (1)$$

where P is the pressure in GPa, $\Delta\lambda$ is the ruby R_1 line shift in nm, and parameter B is 7.665 for quasi-hydrostatic conditions and is 5 for non-hydrostatic conditions. The ruby fluorescence can be conveniently collected using a Raman system such as described below.

To conduct vibrational spectroscopy on materials loaded in DAC effectively, optical transparency is a prime factor in selecting diamond anvils. Two types of diamonds (i.e., type I and type II) are typically used for different spectroscopic probes. Both types have the intense first-order

Raman line at 1332 cm^{-1} (F_{2g} mode of the diamond). The difference between the two types is in the infrared absorption spectrum. Type I anvils (with more nitrogen impurities) have two strong IR absorption regions around 2000 and 1000–1350 cm^{-1}, respectively. In contrast, type II anvils (nitrogen free) have a relatively clean IR window bellow 2000 cm^{-1} allowing effective IR absorption measurements on samples. Therefore, the low-fluorescent type I diamonds are only suitable for Raman spectroscopy, while the type II diamonds are mainly used in IR spectroscopy.

2.2. Raman spectroscopy

Raman spectroscopy is a vibrational spectroscopy based on the inelastic scattering of visible photons (typically from a laser source) by materials, a process with a much smaller cross-section than other spectroscopic processes (e.g., absorption, fluorescence, etc.). Although many commercial Raman microscopy systems are available, they generally have a rigid design that does not allow *in situ* measurements with different DAC configurations. Therefore, a state-of-the-art customized Raman system was constructed to allow the DAC-based measurements in a broad P-T range with multiple excitation laser sources that cover the spectral range from near UV to near IR, such as 488–514 nm lines from an Innova Ar^{+} laser (Coherent Inc.), 532 and 782 mn lines from diode-pumped solid-state lasers, as well as 700–1100 nm lines from a Ti: sapphire laser (Spectral Physics) [10]. Using a 20× Mitutoyo objective, the laser can be focused to less than 5 μm on the sample. The combination of a 15× eyepiece and a digital camera allows precise alignment of the focused laser beam on the sample. With backscattering geometry, the Raman signal is collected by the same objective lens. The elastic Rayleigh scattering is removed by either a pair of notch filters or an edge filter that enabled a spectral range above 100 cm^{-1} to be measured before the total scattered photons are focused on the entrance slit of a spectrometer. The scattered light is then dispersed using an imaging spectrograph (SpectroPro-2500i, Acton Research Corporation) that houses a 0.5 m focal distance monochromator equipped with multiple gratings, such as a 1800 lines/mm grating, allowing a spectral resolution of ±0.1 cm^{-1} to be achieved. The Raman signal was recorded using an ultrasensitive back-illuminated, liquid nitrogen cooled, charge-coupled device (CCD) detector from Acton. The Raman system is first calibrated by using a neon lamp giving an uncertainty of ±1 cm^{-1} before each experiment.

2.3. FTIR spectroscopy

Complementary to Raman spectroscopy, IR absorption spectroscopy provides sensitive and fingerprints information on materials loaded in DAC, especially those with high fluorescence that prohibits effective Raman measurements. The IR measurements for the examples demonstrated in this chapter were mostly carried out using a customized IR micro-spectroscopy system constructed in-house [11]. Specifically, a commercial FTIR spectrometer (model Vertex 80v from Bruker Optics Inc.) containing a Globar IR source constitutes the major component of the micro-IR system. The spectrometer is operated under a vacuum of <5 mbar to efficiently remove the absorption by H_2O and CO_2. The IR beam is collimated with varying diameters achieved by using apertures from 0.25 to 8 mm, and then is directed into a relay box through a KBr window. Using the combination of iris optics and 15× reflective objective lens (numerical

aperture of 0.4), the IR beam is then focused onto the sample in the DAC. Using an XYZ precision stage with the aid of an optical microscope equipped with a 20× eyepiece from Edmond Optics and an objective lens of variable magnifications, the sample loaded in DAC can be easily aligned to allow the maximum transmission of the IR beam. Using a series of iris apertures, the size of the IR beam was set to be identical to the entire sample size (e.g., ~200 μm). Another identical reflective objective as the condenser is used to collect the transmitted IR beam, which is subsequently directed to a midband mercury cadmium telluride (MCT) detector. A ZnSe window equipped on the midband MCT detector allows efficient measurements in the spectral range of 600–12,000 cm^{-1}. The combination of 512 scans and a resolution setting of 4 cm^{-1} is typically used for each spectrum measurement that gives an excellent signal-to-noise ratio. The absorption of diamond anvils loaded with KBr but without any sample is used as the reference spectrum, which is divided as background from each sample spectrum to obtain the absorbance.

2.4. Synchrotron-based FTIR spectroscopy

Synchrotron light is a source of electromagnetic radiation produced by a storage ring housing traveling electrons with a near speed of light. Although synchrotron source provides enormous advantages typically in the X-ray region, the infrared synchrotron light has unique applications for DAC-based measurements due to the very intense, very broad and highly focused IR source that allows very high spatial resolution and far-IR measurements. Some examples in this chapter are based on the experiments performed at the U2A beamline at the National Synchrotron Light Source (NSLS) of Brookhaven National Laboratory (BNL). Briefly, the IR beam from the synchrotron storage ring is first extracted through a wedged diamond window from a source with a 40 × 40 mrad solid angle. Then it is collimated to a 1.5″ diameter beam and directed into a vacuum FTIR spectrometer (Bruker IFS 66V) equipped with three independent microscope systems. The spectrometer is equipped with a number of combinations of IR beam splitters and detectors (e.g., silicon bolometer and MCT). For mid-IR measurements, a Bruker IR microscope is used to focus the IR beam onto the sample. The absorption spectrum is collected in transmission mode by the MCT detector in the spectral range of 600–4000 cm^{-1}. The far-IR spectra are collected using a customized IR microscope allowing very high collection efficiency and recorded by the bolometer in the spectral region of 100 to 600 cm^{-1}. A resolution of 4 cm^{-1} was used in all IR measurements. For all measurements, mid-IR spectra were collected through a 30 × 30 μm^2 aperture, whereas the effective IR transmission area covered the entire sample (i.e., a circle of about 90 μm in diameter) for the far-IR measurements. The data acquisition, processing and analysis are similar to those obtained using the in-house mid-IR spectroscopy system.

3. Pressure-induced conformational change

Pressure-mediated conformational equilibrium is of particular interests because the reactivity of many organic reagents, product yields, and even reaction pathways are strongly correlated

with molecular conformations. Here, two simple halogen substituted alkane molecules, that is, 1,2-dichloroethane (DCE) [12] and chlorocyclohexane (CCH) [13], were investigated under high pressures for conformational and structural changes using *in situ* Raman spectroscopy.

3.1. 1,2-Dichloroethane

As a model molecule, DCE has two representative conformations, that is, *gauche* and *trans* depending on the relative orientations of the halogens attached to the two carbons, making it an interesting candidate for conformational studies under high pressures. At pressures below 0.6 GPa, fluid DCE exhibits two conformations, that is, *gauche* and *trans* in equilibrium. Upon compression, the equilibrium appears to shift toward *gauche* conformation (**Figure 2**). Upon further compression, DCE was found to transform to a solid phase with exclusive *trans* conformation. In fluid phase, all the characteristic Raman shifts remain constant whereas in the solid phase they move to higher frequencies with increasing pressure. At about 4–5 GPa, DCE transforms into a crystalline phase from a possible disordered phase as indicated by the appearance of several new lattice modes and bandwidth narrowing. Dramatic changes in Raman spectra of DCE were observed when compressed to ~8–9 GPa. For instance, the C—C—Cl bending mode at 325 cm^{-1} splits, the inactive internal mode at 684 cm^{-1} becomes observable, and new lattice modes appear. All these observations suggest another pressure-induced phase transformation. Significant changes in pressure dependence of representative Raman modes at the distinctive pressures further confirm the transition and allow the identification of phase boundaries. Although with a likely lower symmetry, the new phase remains crystalline. The transformations are found reversible in the entire pressure region upon decompression. Quantitative analysis on Raman intensities associated with each conformer even allows the determination of the transformation volume of 0.58 ± 0.10 cm^3/mol (**Figure 3**).

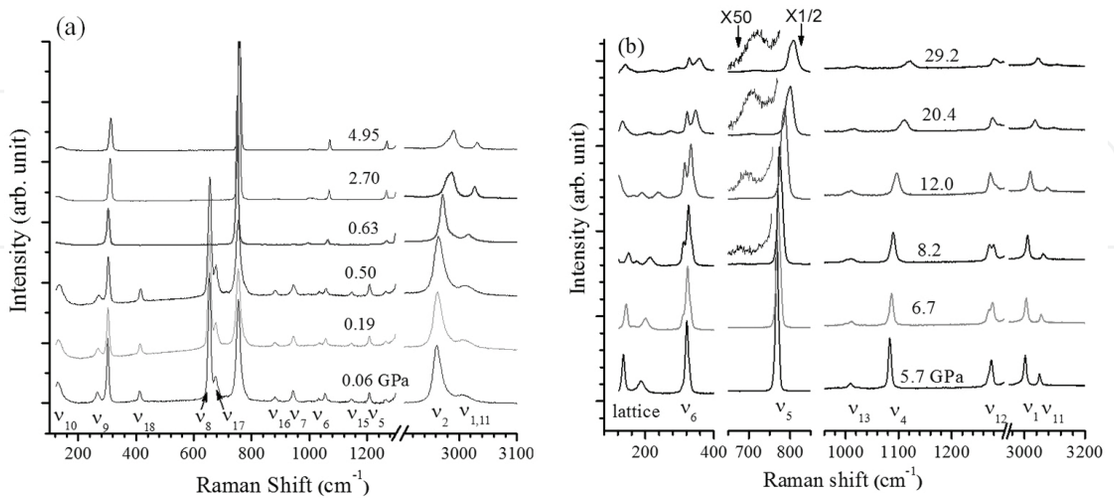

Figure 2. Representative Raman spectra of DCE on compression in the pressure region of (a) 0–5.0 GPa and (b) 5.7–29.2 GPa and the spectral region of 120–1300 cm^{-1} and 2900–3100 cm^{-1}. The assignments of Raman active mode are labeled below for *gauche* (a) and *trans* (b) conformations. Reproduced with permission from reference [12].

http://dx.doi.org/10.5772/64617

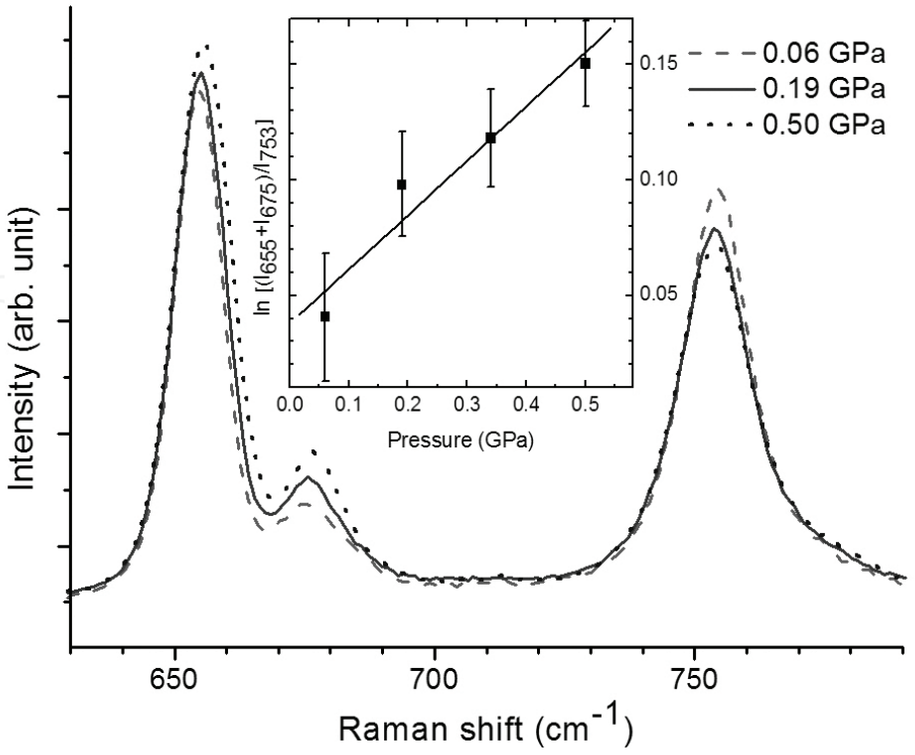

Figure 3. Representative Raman spectra of DCE in the magnified spectral region of 600–800 cm^{-1} for fluid phase. The inset is the plot of logarithm of relative intensities of the first two peaks over the third peak as a function of pressure. Reproduced with permission from reference [12].

3.2. Chlorocyclohexane

In situ Raman measurements on CCH at room temperature and high pressures up to 20 GPa also show interesting pressure-dependent conformational changes [13]. Below 0.7 GPa, CCH exists as a fluid phase with a mixture of axial and equatorial conformations in equilibrium, which is shifted to axial upon compression (**Figure 4a**). The shift was attributed to the smaller volume of axial conformer with a volume difference of −2.2 cm^3 mol^{-1} relative to equatorial conformation, which is consistent with previous studies. When compressed to 2.4 GPa, the depletion of C—H stretching mode at high frequency as well as the splittings of the ν_{22} mode suggest a phase transition (**Figure 4b**). The splittings are further enhanced at 4.8 GPa together with the observation of a new lattice mode, suggesting another phase transition. Upon careful comparison, these high-pressure phases are likely different from the low-temperature phases observed previously. Significant broadening of Raman profiles was observed above 9.5 GPa, indicating that CCH is undergoing gradual disordering at high pressures (**Figure 4b**). Upon releasing of pressure, CCH is fully recoverable indicating that the six-member ring can sustain high pressures up to 20 GPa. The observation of two new modes upon decompression, however, suggests that phase transformation of CCH is partially irreversible above 2.5 GPa. The phase produced by decompression exhibits a contribution from axial conformation of CCH. These pressure-induced hysteresis and partial irreversibility can be attributed to the plastic nature of the CCH crystals.

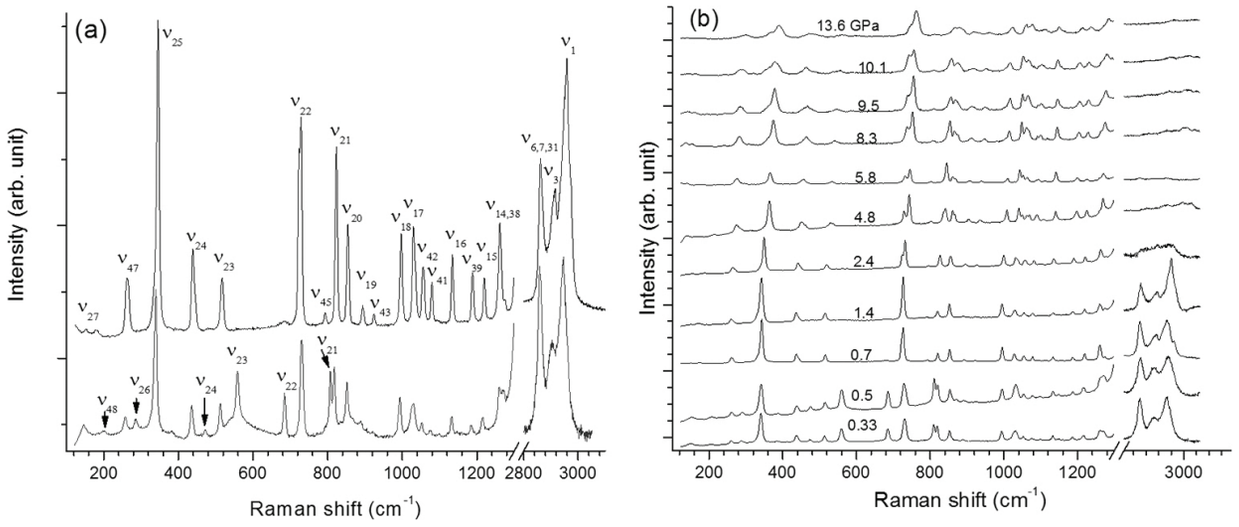

Figure 4. (a) Raman spectra of CCH collected at ambient pressure (top) in comparison with that collected upon slight compression (i.e., at 0.03 GPa, bottom). CCH exists as a mixture of axial and equatorial conformer with the latter dominant at condition and thus the assignment labeled above each Raman modes refers to equatorial conformation for the top spectrum. Axial and equatorial conformers share majority of common Raman modes and thus only those exclusively associated with axial conformer are labeled in the bottom spectrum. (b) Selective Raman spectra of CCH on compression in the pressure region 0–14 GPa in the spectral range of 120–1300 cm^{-1} and 2800–3200 cm^{-1}. Reproduced with permission from reference [13].

4. Pressure-mediated hydrogen bonding

Hydrogen bonding plays an important role in stabilizing a wide range of molecular structures and influences the chemical and physical properties of molecular systems. Typically, the characterizations of hydrogen bonding are inferred from crystal structures or by theoretical modeling. Here two examples are shown to demonstrate that vibrational spectroscopy on materials loaded in DAC can reveal interesting pressure-mediated hydrogen bonding interactions.

4.1. Ethylene glycol

Ethylene glycol (EG) serves as a prototype for understanding hydroxyl group interactions in biological compounds such as sugars and polysaccharides. Using *in situ* high-pressure Raman and infrared absorption spectroscopy, the structural and conformational transformations of EG were found to be substantially influenced by hydrogen bonding interactions under pressure up to 10 GPa [14]. The high-pressure behavior of Raman modes suggests that EG exists as a liquid with a mixture of *trans* and *gauche* conformations up to 3.1 GPa. In the pressure range 4–7 GPa, the solid phase has a varied proportion of *trans* and *gauche* conformations. At pressures above 7 GPa, the EG structure is stabilized to *gauche* conformation and remains stable up to 10 GPa. The increase in the intensity and the large pressure induced red shift of the infrared active OH mode ν_ε suggest that intra-molecular hydrogen bond is formed and

strengthened during the stabilization of *gauche* conformation (**Figure 5**). The observed pressure induced changes were found to be completely reversible on decompression to ambient conditions.

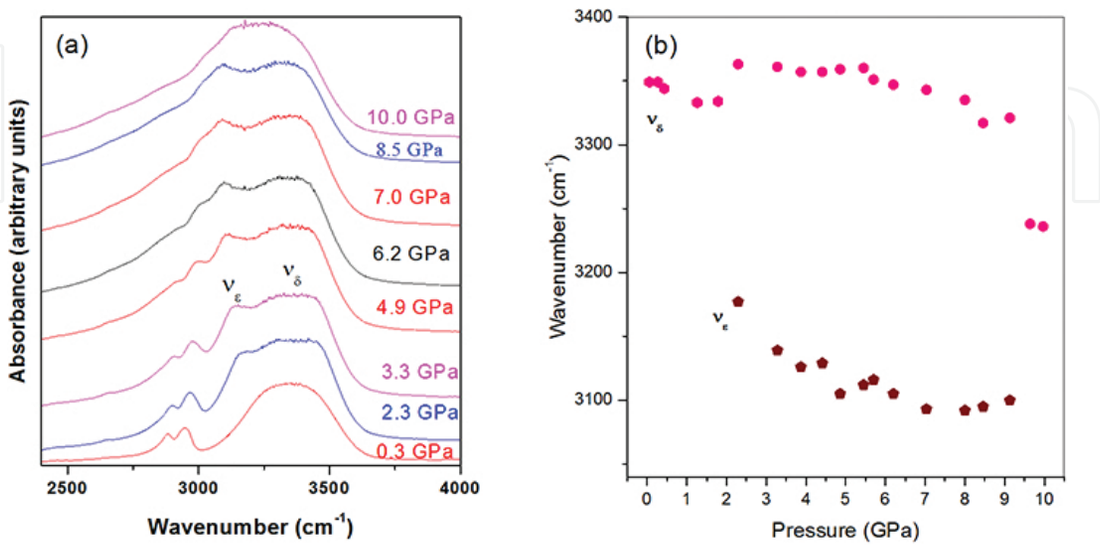

Figure 5. Infrared absorption spectra of ethylene glycol at different pressures under compression in the spectral region of 2500–4000 cm^{-1} (a) and variation of OH stretching infrared active modes of ethylene glycol with pressure (b). Reproduced with permission from reference [14].

4.2. Bis(1H-tetrazol-5-yl)amine monohydrate

Bis(1H-tetrazol-5-yl)amine (BTA) with two tetrazole rings linked by one nitrogen atom that contains 82.5 wt% nitrogen has been considered a promising high energy density material. Moreover, examining the possibility of converting this high nitrogen content precursor to other polymorphs with higher energy density using high pressure is of great interest. *In situ* high-pressure study of BTA·H_2O was carried out up to 25 GPa at room temperature using Raman and IR spectroscopy, X-ray diffraction as well as *ab initio* simulations [15]. Upon compression, both the Raman and IR vibrational bands were found to undergo continuous and gradual broadening without significant change of the profile, indicating pressure-induced structural disordering rather than phase transition. X-ray diffraction patterns confirmed the pressure effect on the structural evolutions of BTA·H_2O. Interestingly, in contrast to all other Raman and IR modes of BTA·H_2O which exhibit blue shifts, the N-H stretching mode shows a prominent red shift upon compression to ~8 GPa, strongly suggesting pressure enhanced hydrogen bonding between BTA and H_2O (**Figure 6**). The analysis of X-ray diffraction patterns of BTA·H_2O indicates that the unit cell parameters undergo anisotropic compression rate. The pressure dependence of the unit cell parameters and volumes coincides with the behavior of the hydrogen bonding enhancement (**Figure 7**). Aided with first-principles simulations, these pressure-mediated structural modifications consistently suggest that hydrogen bonding played an important role in the compression behavior and structural stability of BTA·H_2O under high pressures (**Figure 8**).

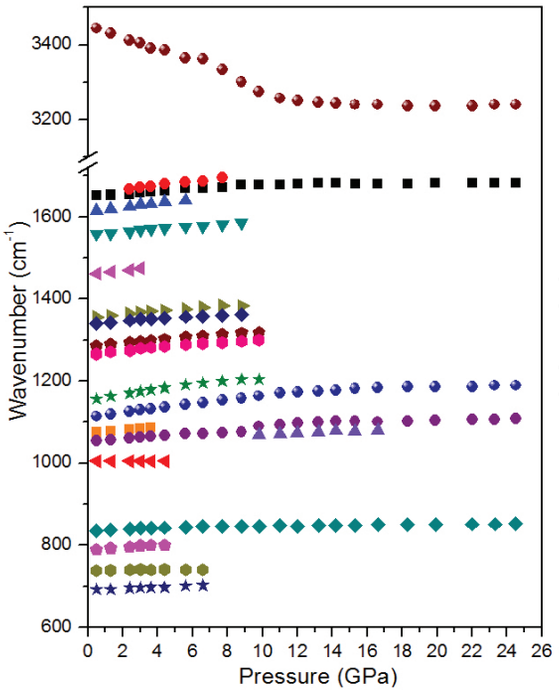

Figure 6. Pressure dependence of IR modes of BTA·H_2O on compression. Reproduced with permission from reference [15].

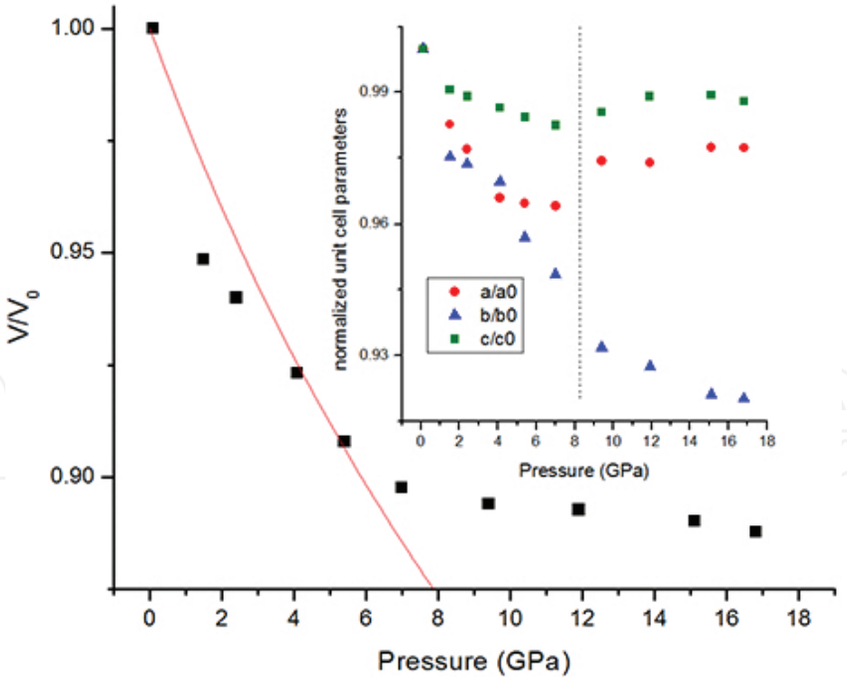

Figure 7. Normalized unit cell volume versus pressure (black squares) for BTA·H_2O on compression and fitted equation of state (red curve) using second-order Birch-Murnaghan equation. The inset shows normalized monoclinic unit cell parameters for *a, b* and *c* of BTA·H_2O on compression. The vertical dashed line denotes the pressure at which the monotonic contraction of *a* and *c* axes changed. Reproduced with permission from reference [15].

http://dx.doi.org/10.5772/64617

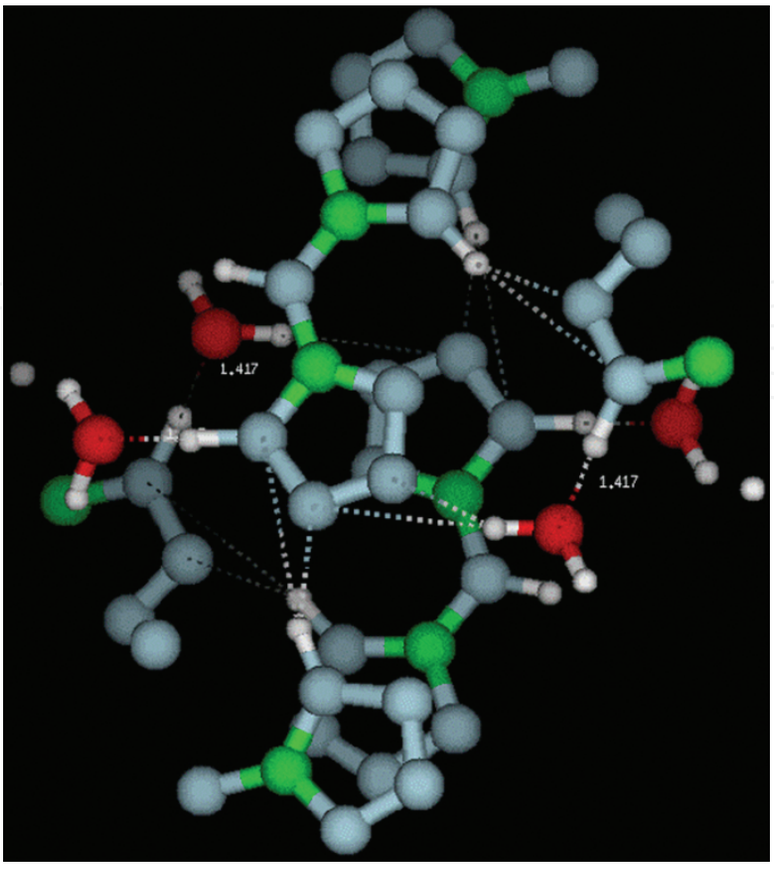

Figure 8. Proton hopping and molecular interactions of BTA·H_2O system based on first-principles simulations.

5. Structural and phase transitions

5.1. Boron nitride nanotubes

Compared to carbon nanotube, boron nitride nanotube (BNNT) has structure-independent wide band gap, enhanced thermal stability, high resistance to oxidation at high temperatures, high thermal conductivity and remarkable yield strength, making it a promising advanced material for a wide range of applications. Multiwalled boron nitride nanotubes (BNNTs) were compressed at room temperature in diamond anvil cells up to 35 GPa followed by decompression and characterized by *in situ* FTIR absorption spectroscopy [11]. Pressure-induced transformations from a hexagonal to a more closely packed wurtzite structure were observed at 11 GPa, which is similar to that reported for bulk BN (**Figure 9**). However, BNNTs exhibit quantitative differences compared to bulk h-BN in terms of transformation completeness and reversibility (**Figure 10**). These findings provide strong evidence that significantly different yield of sp^3 bonding formation originated from different morphologies of the starting BN materials (**Figure 11**). The unique transformation mechanism for BNNTs provides new useful information for developing BNNTs as potential advanced materials with more desirable properties than carbon nanotubes.

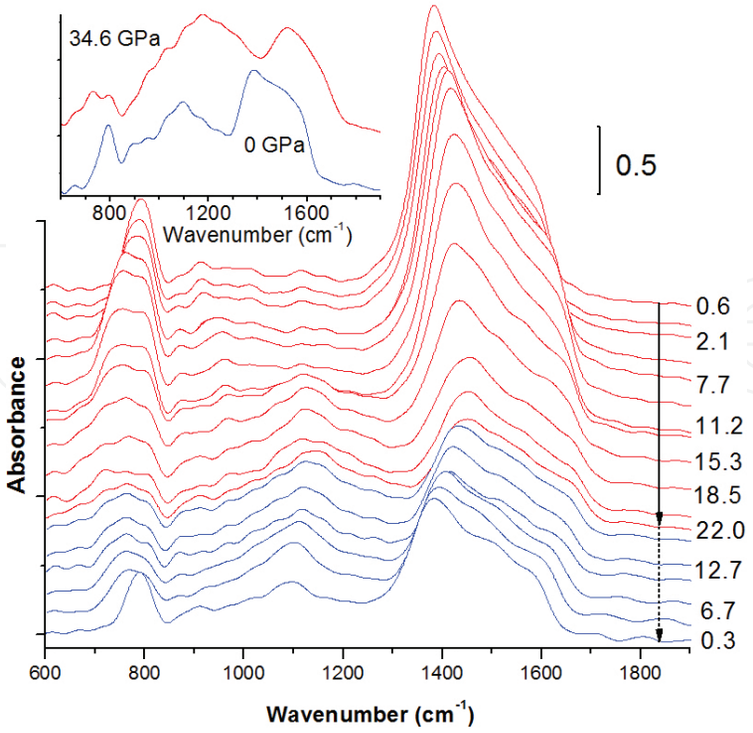

Figure 9. Infrared spectra of BNNTs at selected pressures upon compression (red lines) and decompression (blue lines) in the spectra region of 600–1900 cm^{-1}. The solid and dashed arrows indicate the compression and decompression sequence. The inset shows spectra from another run at a highest pressure of 34.6 GPa on compression (red line) and complete pressure release (blue line). Reproduced with permission from reference [11].

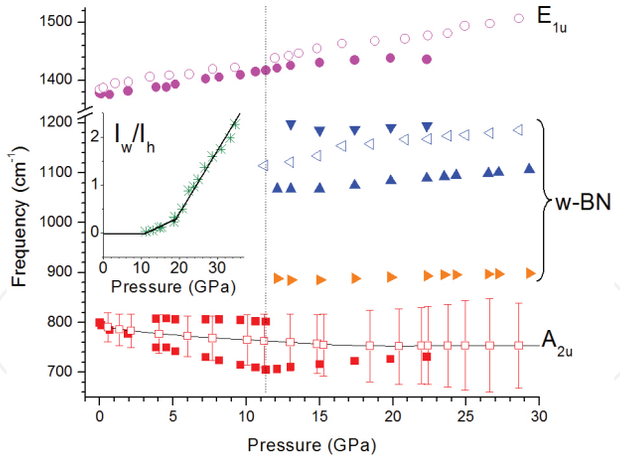

Figure 10. Pressure dependence of representative IR modes of BNNTs (open symbols) and in comparison with those for bulk h-BN (solid symbols) on compression. The squares and circles are the respective A_{2u} and E_{1u} modes of h-BN structure, while other symbols represent IR modes for w-BN structure. The dashed line at around 11 GPa denotes the transition onset for both BNNTs and bulk h-BN. The vertical bars for A_{2u} mode represent the full width at half maximum for BNNTs. The inset shows the ratio of the IR band intensity of the mode at 1125 cm^{-1} for w-BN over the E_{1u} mode for h-BN observed in BNNTs labeled as I_w/I_h. The solid lines are for eye guidance showing three distinctive conversion regions. Reproduced with permission from reference [11].

http://dx.doi.org/10.5772/64617

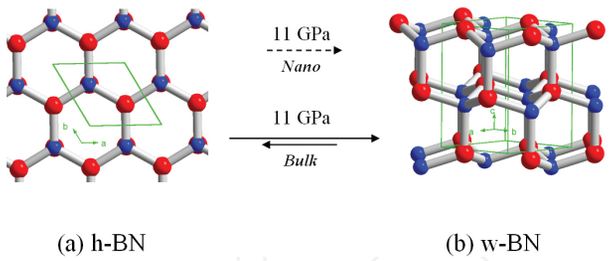

Figure 11. Crystal structures and bonding patterns of (a) h-BN and (b) w-BN with the transformation conditions for BNNTs and bulk h-BN denoted. The red and blue balls represent boron and nitrogen, respectively. The dashed arrow for BNNT indicates incomplete irreversible transformation, while the solid arrows with different length for bulk h-BN indicate partial reversibility. Reproduced with permission from reference [11].

5.2. Aromatic compounds

Aromatic compounds have been investigated under non-ambient conditions over the past few decades due to their great importance in both fundamental and applied science. In particular, they have been widely studied in chemical synthesis under elevated temperatures and pressures as the precursors of technological materials, such as amorphous solids and conjugated polymers [16]. For instance, using *in situ* Raman spectroscopy and infrared absorption spectroscopy, structural transitions of pyridine have been investigated as a function of pressure up to 26 GPa [17]. By monitoring the band profiles in both Raman and IR spectra and especially the Raman shifts in the lattice region, a liquid-to-solid transition at 1 GPa followed by solid-to-solid transitions at 2, 8, 11 and 16 GPa were observed upon compression (**Figure 12**). All these transitions were reversible upon decompression from 22 GPa. When compressed beyond 22 GPa, a further chemical transformation was observed which is evidenced by the substantial and irreversible changes of the Raman and infrared spectra. This transformation could be attributed to the destruction of the ring structure. The high-pressure behavior of pyridine was also compared to that of benzene. The similar transition sequence with well-aligned transition pressures indicates that aromatic compounds with isoelectronic structures may have similar structural stabilities and thus transition behaviors under high pressure.

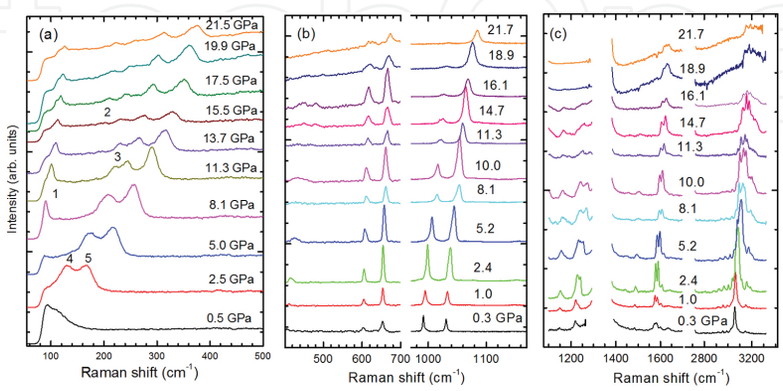

Figure 12. Selected Raman spectra of pyridine on compression in the spectral region of 60–500 cm^{-1} (a), 400–1160 cm^{-1} (b) and 1100–3300 cm^{-1} (c). Reproduced with permission from reference [17].

5.3. Metal and chemical hydrides

High-pressure investigations of potential hydrogen storage materials, especially hydrogen-rich metal and chemical hydrides have received increasing attentions [8]. Not only has pressure demonstrated great promises for producing new structures and materials but also many known hydrogen-rich materials have exhibited new transformations as well as totally different thermodynamic and kinetic behaviors under higher pressures than under ambient conditions. Hydrides in a wide range of different categories, such as calcium borohydride, sodium amide and ammonia borane, have been extensively investigated under high pressures by vibrational spectroscopy, X-ray diffraction and theoretical calculations [18–21]. Here ammonia borane (NH_3BH_3) is chosen as an example to demonstrate that vibrational spectroscopy can be an effective tool to elucidate novel high-pressure structures [18, 21].

Using *in situ* Raman and synchrotron IR spectroscopy, the pressure behavior of ammonia borane complex as a promising hydrogen storage material was investigated up to 14 GPa [18]. In the low-pressure region (<2 GPa), the complex was found to undergo a structural transformation to, an ordered, possibly orthorhombic structure from originally a disordered tetragonal phase. With increasing pressure, the Raman and IR spectra suggest several solid-to-solid transformations at about 2.4, 5.5, 8.5 and 10.4 GPa, as evidenced by the distinctive profiles and the pressure dependences of characteristic modes (**Figure 13**). Upon decompression, these pressure-induced transformations are found completely reversible with intact chemical structure of the NH_3BH_3 complex, but possible modifications to the crystal structures. Analysis of combined Raman and IR measurements, especially the lattice features (**Figure 13a**), suggests that NH_3BH_3 structures below 5.5 GPa resemble a low-pressure orthorhombic structure, while in the higher pressure regions, NH_3BH_3 complexes may undergo transformations to disordered or amorphous structures.

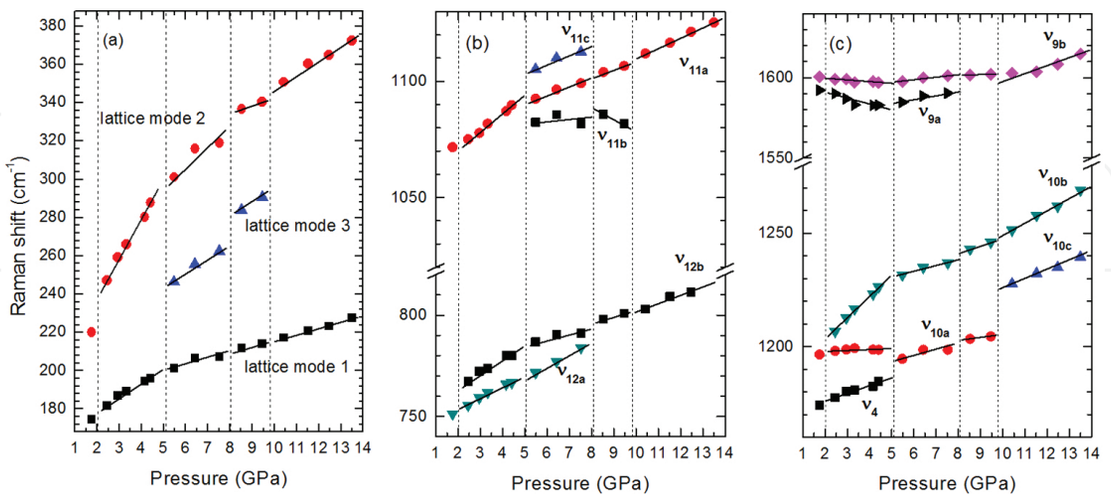

Figure 13. Pressure dependences of Raman shift of NH_3BH_3 on compression for (a) the lattice modes; (b) the ^{11}B-N/^{10}B-N stretch (ν_5/ν_5') modes; and (c) the NBH rock (ν_{12a}, ν_{12b}, ν_{11a}, ν_{11b} and ν_{11c}) modes. The solid lines crossing the solid symbols are based on linear fit. The vertical dashed lines indicate the proposed phase boundaries. Reproduced with permission from reference [18].

http://dx.doi.org/10.5772/64617

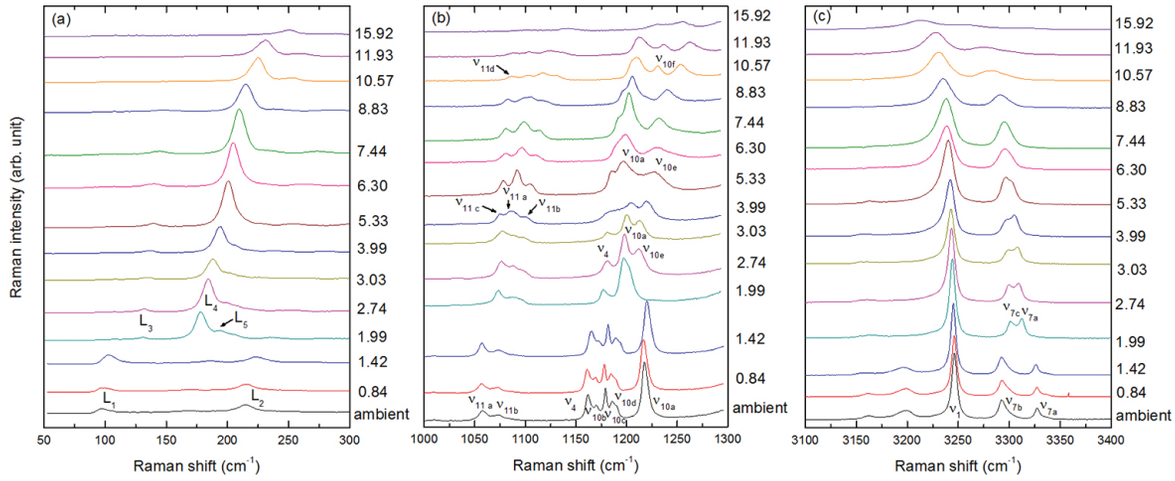

Figure 14. Selected Raman spectra of NH_3BH_3 collected on compression up to 15.92 GPa at 180 K in the region of 50–300 cm^{-1} (a), 1000–1300 cm^{-1} (b), and 3100–3400 cm^{-1} (c). The assignments are labeled for selected Raman mode at selected pressures. Reproduced with permission from reference [21].

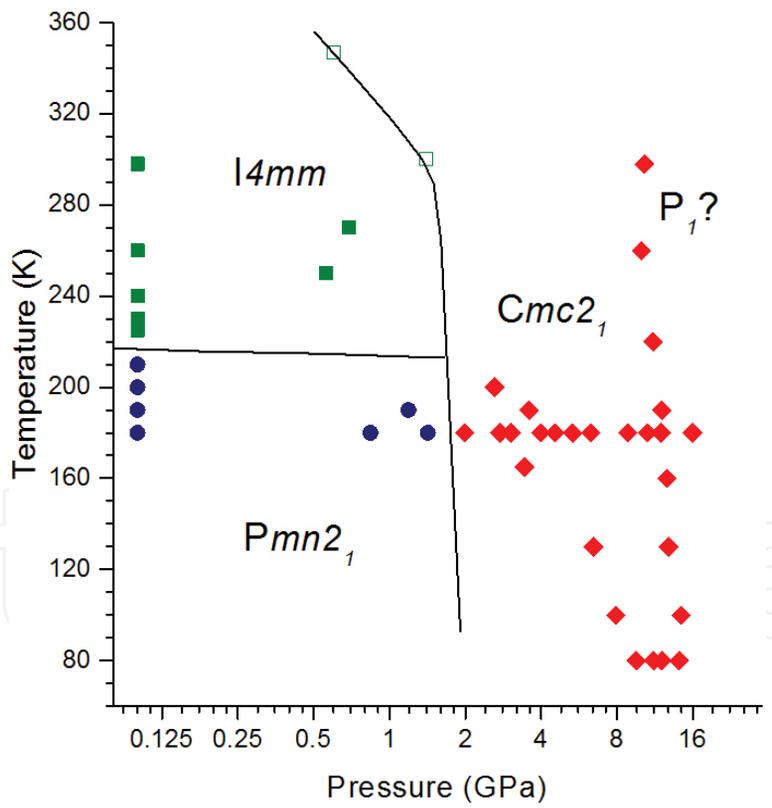

Figure 15. Schematic P-T phase diagram of NH_3BH_3 in the pressure region of 0–15 GPa (in $\log_2$ scale) and temperature region of 80–350 K. Solid symbols are experimental data from this study, with squares for *I4mm* phase, circles for *Pmn*2$_1$ phase and diamonds for *Cmc*2$_1$ phase. The open squares are adopted from reference [22]. The solid lines denote the rough boundaries among the three known phases. The *P*1 phase labeled is considered tentative. Reproduced with permission from reference [21].

Subsequently, ammonia borane was investigated at simultaneous high pressures (up to 15 GPa) and low temperatures (down to 80 K) by *in situ* Raman spectroscopy [21]. Upon cooling to 220 K from room temperature at ambient pressure, ammonia borane transforms from *I*4*mm* to $Pmn2_1$. Upon isothermal compression to 15 GPa at 180 K, another three pressure-induced structural transformations were observed. These transitions can be evidenced by the change in the Raman profile as well as the pressure dependence of the major Raman modes (**Figure 14**). Upon decompression and warming-up, these P-T-induced transformations are found completely reversible. With the aid of factor group analysis, the phases above 1.5 GPa were found consistent with the crystal structure with space group $Cmc2_1$, and that the transitions at 5 and 8 GPa are second order in nature, which can be interpreted as enhanced inter-molecular interactions within the same or possibly a slightly modified crystal lattice. Further compression above 15 GPa leads to the gradual transformation to an amorphous phase. When combined with previously reported high-pressure and room-temperature data, our Raman measurements from multiple runs covering various P-T paths allowed the significant update of the P-T phase diagram of ammonia borane in the pressure range of 0–15 GPa and the temperature range of 80–350 K (**Figure 15**).

6. Pressure-induced chemical reactions

6.1. Acrylic acid

Pressure-induced polymerization is a chemical process pertaining to green chemistry as the reactions can be carried out in the absence of any solvent or catalyst, which implies a lesser environmental impact. Poly(acrylic acid) is a well-known polymer with a wide variety of industrial applications such as being super absorbent materials, biocompatible polymers, polyelectrolytes and nanopolymers in molecular devices. Therefore, it is very significant in the polymer industry to explore pressure-induced polymerization from this monomer, as the polymer product with improved properties distinct from that obtained using conventional synthetic methods might be obtained. The first pressure-induced structural and polymeric transformations of acrylic acid were studied by *in situ* Raman spectroscopy [23]. Upon compression to 0.3 GPa, a liquid-to-solid transformation was observed, followed by a solid-to-solid transition at ~2.7 GPa. The two new high-pressure crystalline phases are labeled as phase I and II, respectively (**Figure 16a**). Phase I had a possibly similar structure that resembles low-temperature phase reported previously. Phase II can be interpreted as a denser phase with strong intermolecular interactions leading to polymerization or oligomerization ultimately. When compressed to above 8 GPa, acrylic acid transforms into a disordered polymeric phase (**Figure 16b**). Upon decompression to ambient pressure, the retrieved polymeric phase exhibits a significant amount of acrylic acid monomers or oligomers. Comparative Raman measurements on standard commercial poly(acrylic acid) (**Figure 17**) allowed the understanding of possible structures of the polymeric phase of acrylic acid produced in this study. Overall, our analysis suggests that hydrogen bonding played a significant role in the pressure-induced polymerization/oligomerization process.

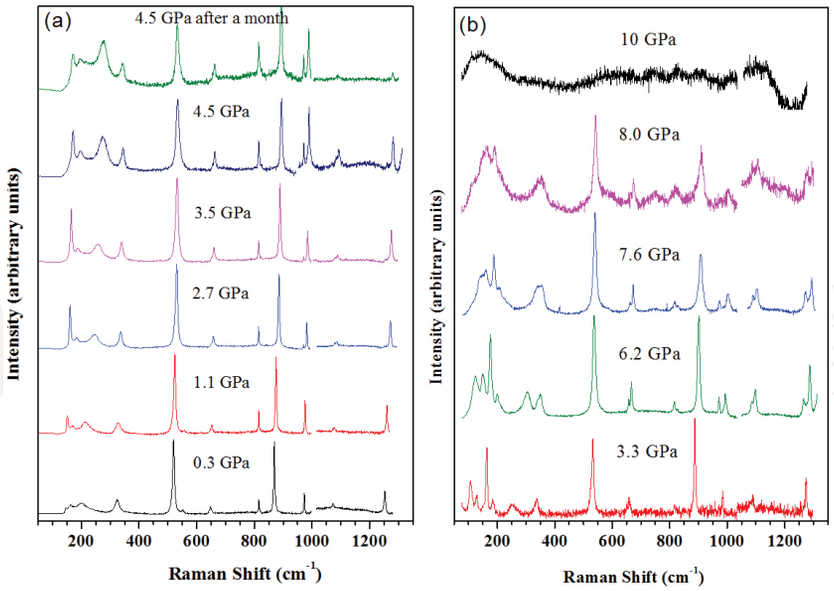

Figure 16. Raman spectra of acrylic acid at selected pressures upon compression in the pressure region of 0.3–4.5 GPa (a) and 3.3–10 GPa (b) in the spectral region of 100–1300 cm^{-1}. Reproduced with permission from reference [23].

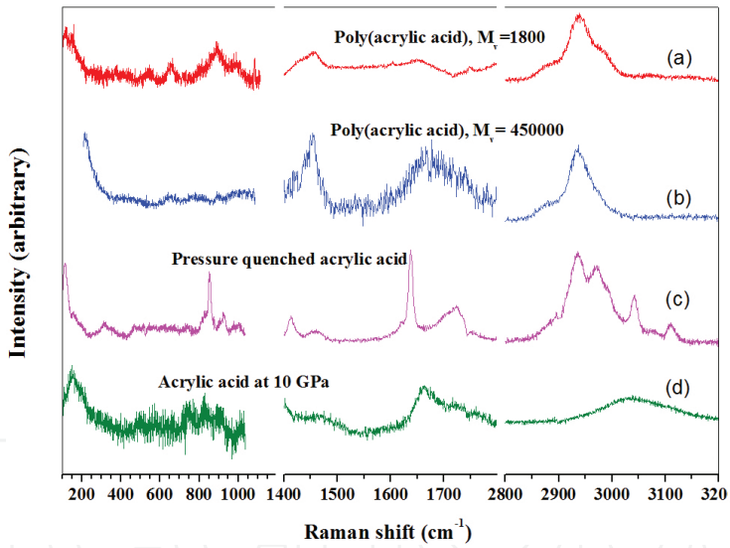

Figure 17. Raman spectrum of poly(acrylic acid) purchased from Aldrich with an average molecular weight of 1800 g/mol (a) and 450,000 g/mol (b) in comparison with that of recovered acrylic acid by decompression from 10 GPa (c) and that of acrylic acid at 10 GPa (d). Reproduced with permission from reference [23].

6.2. Ethylene glycol

Using combined high-pressure and photon excitations especially in the UV range has demonstrated strong potential to produce new molecular materials in a highly efficient way. Using multi-line UV radiation at ~350 nm, the photon-induced reactivity of liquid ethylene glycol (EG) at room temperature was investigated by FTIR spectroscopy [24]. Upon UV irradiation,

IR spectra of EG show two sets of distinctive profiles after specific reaction time, indicating multiple photon-induced chemical reactions, which can be designated as primary and secondary processes (**Figure 18**). Careful spectral analysis allows the identification of primary reaction products that include glycolaldehyde, acetaldehyde and methanol. Further photoreactions of these primary products led to the formation of the secondary products, which were identified as methane, formaldehyde, methoxymethanol, methylformate and carbon dioxide. Based on these reaction products, possible reaction mechanisms and production pathways were proposed. We also found that the initial loading pressure of EG plays an important role in influencing the reaction kinetics as well as in controlling the accessibilities for some reaction channels such as for CH_4 (**Figure 19a**). Quantitative analysis of the antisymmetric stretching mode of CO_2 formed at different loading pressures suggests the formation of CO_2 clathrate hydrates well as CO_2 clusters. The stabilities as well as relative abundance of these CO_2 species are found to be dependent on both pressure and radiation time (**Figure 19b**). These observations revealed interesting pressure-induced CO_2 sequestration behaviors as a result of photochemical reactions of ethylene glycol.

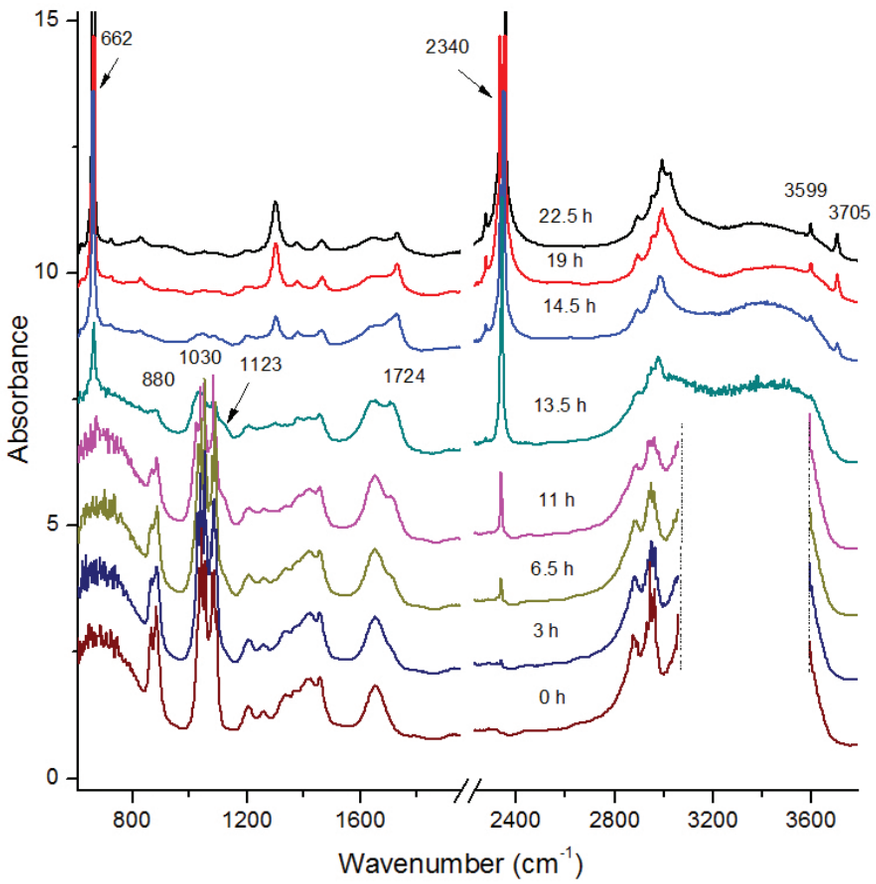

Figure 18. Selected FTIR spectra of EG with an initial loading pressure of 0.1 GPa upon UV irradiation (with λ of ~350 nm and power of ~700 mW) collected at different radiation time. The most characteristic new IR bands emerged at 13.5 h and observed at 22.5 h indicating sequential photochemical reactions are labeled. The spectral region in 3000–3500 cm^{-1} before 13.5 h is truncated due to the saturated IR absorption intensity. Reproduced with permission from reference [24].

http://dx.doi.org/10.5772/64617

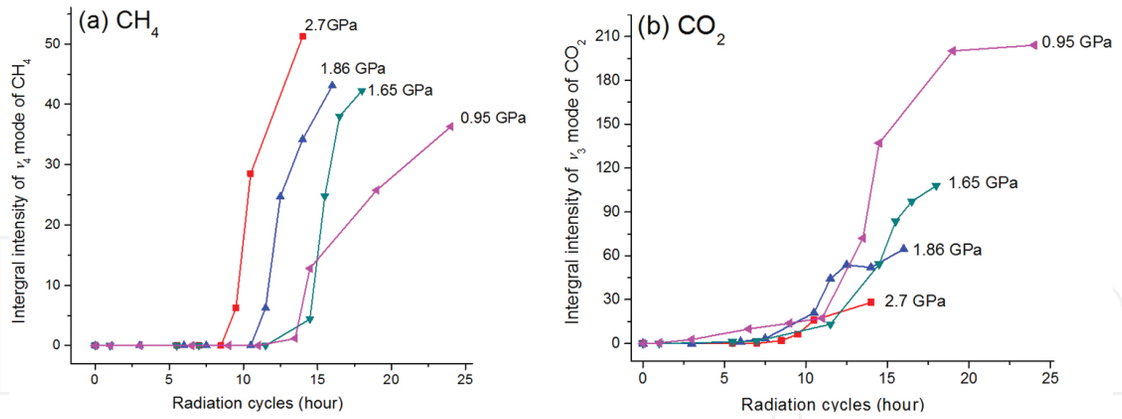

Figure 19. Relative photochemical reaction yields of CH_4 (a) and CO_2 (b) derived by integrating the intensity of the respective characteristic IR modes (ν_4 of CH_4 and ν_3 of CO_2) as a function of radiation time for EG samples with an initial loading pressure of 0.1, 0.5, 1.0 and 2.0 GPa. The pressures labeled for each sample indicate the final system pressure. Reproduced with permission from reference [24].

7. Porous materials and guest-host interactions

7.1. ZIF-8

ZIF-8 is a representative member of the zeolitic imidazolate framework (ZIF) family, an emerging class of porous materials with promising applications in gas storage and catalysis, etc. As a result, substantial interest has been focused on the investigation of its structure and properties under different conditions. Pressure tuning has proven an important and effective means to modify the structures and thus the associated properties of porous materials. Therefore, ZIF-8 was investigated under high pressures up to ~39 GPa using *in situ* IR spectroscopy [25]. Upon compression to 1.6 GPa followed by decompression, the structural modifications on ZIF-8 framework appear reversible (**Figure 20a**). However, further compression to higher pressures led to irreversible structural transitions to an amorphous phase characterized by the very broad IR profiles (**Figure 20b**). Nevertheless, the chemical structure of the framework was found to sustain extreme compression without permanent breaking down. Overall, the high-pressure behavior and especially the surprising chemical stability probed by *in situ* IR spectroscopy demonstrate strong promises storage applications of ZIF-8 under extreme conditions.

In a subsequent study, ZIF-8 framework was investigated when loaded with CO_2 in a diamond anvil cell at high pressures of 0.8 GPa, far beyond the conventional gas adsorption pressure also using *in situ* FTIR spectroscopy [26]. Upon loading, CO_2 molecules in two types of environment (i.e., outside as bulk medium and inside the framework) can be unambiguously differentiated by monitoring the combination IR bands of CO_2 (**Figure 21**). Furthermore, pressure was found to play a regulating role in the migration of CO_2 molecules with respect

to the framework even at room temperature. The strong interactions between CO_2 and framework are evident from the IR features of the framework (e.g., C═C stretching region), providing valuable information about the possible interaction site. As guest molecules, CO_2 in turn can substantially enhance the structural stability of the ZIF-8 framework as compared to the empty framework (**Figure 22**). The enhanced CO_2 storage capacity of ZIF-8 at high pressure provides new insight into the gas capture and storage applications of ZIFs.

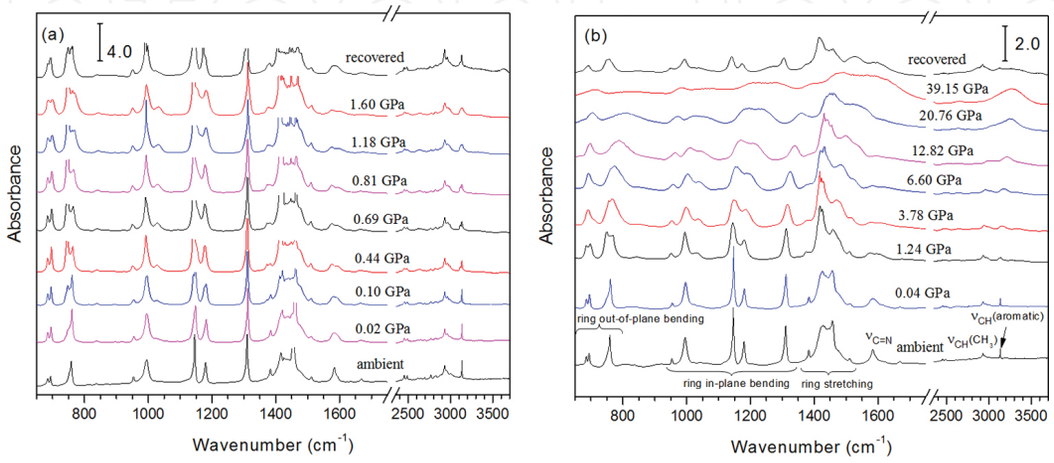

Figure 20. Selected IR spectra of ZIF-8 on compression to a highest pressure of 1.60 GPa and as recovered (a), and to another highest pressure of 39.15 GPa and as recovered (b). Reproduced with permission from reference [25].

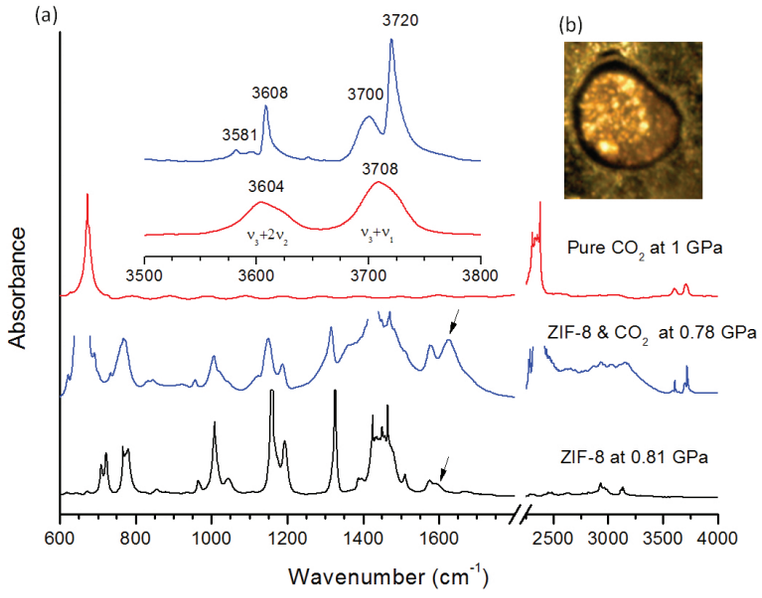

Figure 21. (a) The comparison of IR spectrum of pure CO_2 (top), ZIF-8 loaded with CO_2 (middle) and that of pure ZIF-8 (bottom) at similar pressures. The inset shows the spectral region for the combination modes of CO_2 loaded with ZIF-8 loaded (top) and pure CO_2 (bottom). (b) Photograph of ZIF-8 loaded with CO_2 obtained under an optical microscope. The arrows denote the positions of the C═C stretching mode of the imidazole ring. Reproduced with permission from reference [26].

http://dx.doi.org/10.5772/64617

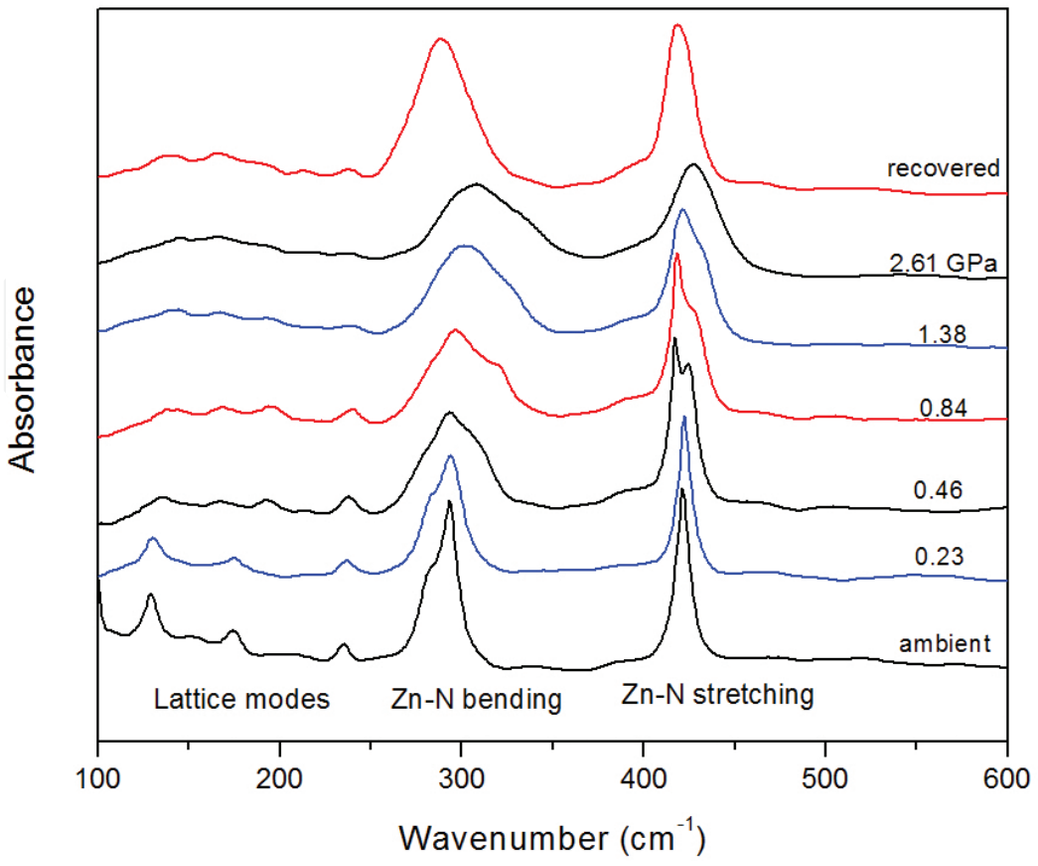

Figure 22. Far-IR spectra of empty ZIF-8 framework upon compression to 2.61 GPa and decompression to ambient pressure. These far-IR spectra suggest that pressure can significantly modify the crystal structures of empty ZIF-8 framework irreversibly. Reproduced with permission from reference [26].

7.2. MIL-68

As a promising candidate for the application of gas storage and separation, metal-organic framework (MOF) MIL-68 has unique structural topology that contains two types of channels with distinct pore sizes. Using *in situ* IR spectroscopy, the behavior of as-made and activated MIL-68 (In) and their structural reversibilities were investigated under high pressures [27]. Overall, the structures of both frameworks were found highly stable upon compression to 9 GPa. However, some modifications on the local structure especially the bridging O—H units, which are very sensitive to compression, can be clearly identified. The structural modifications are found to be completely reversible upon decompression for as-made MIL-68 (In) but irreversible for the activated framework. The different reversibility of framework is most likely associated with the solvent DMF molecules contained in the framework channels. Furthermore, the stability of the activated framework was investigated using PTM to achieve hydrostatic compression. The pressure-induced inclusion of PTM makes the framework more resilient to compression (18 GPa). As a result, structural modifications of the framework with PTM are completely reversible upon decompression (**Figure 23a**). Moreover, the performance of MIL-68 (In) for CO_2 adsorption under high

pressure was investigated. Our results show that at relative low pressures such as below 0.35 GPa, the hexagonal pores are readily accessible for CO_2, while the triangular pores become accessible for CO_2 at higher pressures such as above 1.5 GPa (**Figure 23b**). Such pressure-regulated CO_2 occupation in different channels of the MIL-68 framework is completely reversible between compression and decompression (**Figure 23c**). The unique adsorption behavior of CO_2 in the MIL-68 is strongly correlated with the OH units contributing as the primary binding sites through hydrogen bonding with CO_2. Molecular dynamics simulations further support our analysis (**Figure 24**). The high framework stability and enhanced CO_2 adsorption of MIL-68 (In) under high pressure make it a promising candidate for greenhouse gas storage.

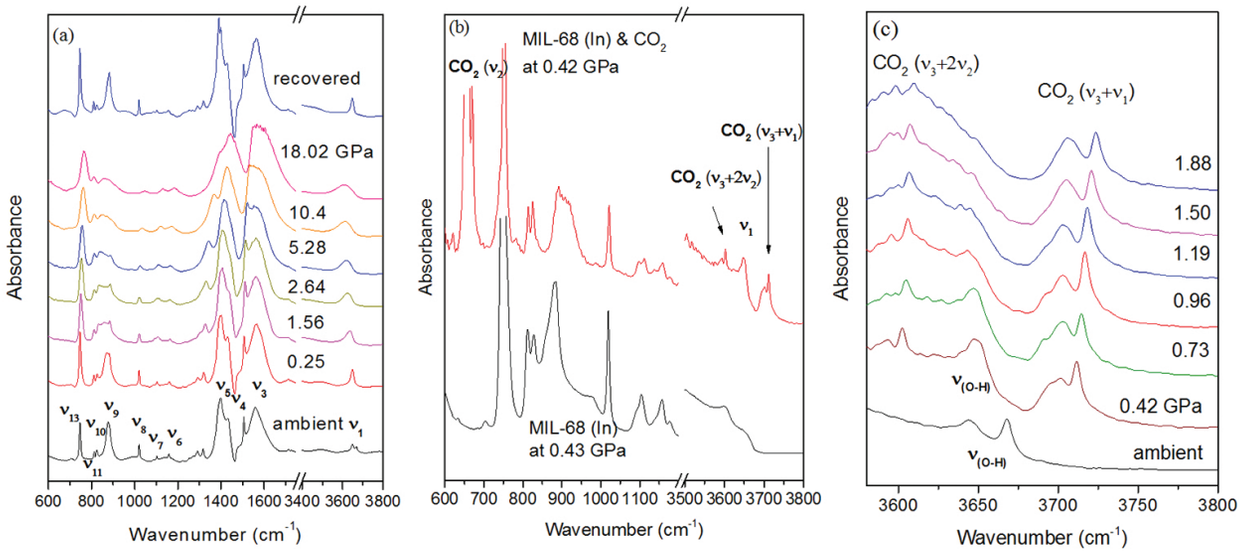

Figure 23. (a) IR spectra of activated MIL-68 (In) with PTM upon compression. (b) IR spectra of activated MIL-68 (In) and MIL-68 (In) loaded with CO_2 at around 0.4 GPa in the frequency region of 600–3800 cm^{-1}. (c) IR spectra of MIL-68 (In) loaded with CO_2 upon compression. Reproduced with permission from reference [27].

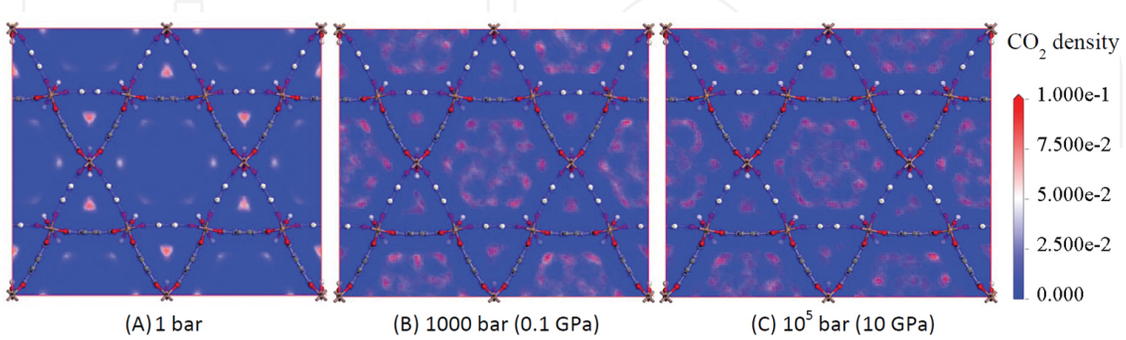

Figure 24. Simulated contour plots of the CO_2 probability density distributions along the hexagonal and triangular channels of MIL-68 (In) framework at (a) 1 bar, (b) 1000 bar or 0.1 GPa and (c) 10^5 bar (or 10 GPa). Reproduced with permission from reference [27].

http://dx.doi.org/10.5772/64617

8. Summary and future perspectives

In summary, this chapter demonstrated the application of *in situ* vibrational spectroscopy including Raman and FTIR spectroscopy in the elucidation of molecular structures and transformation mechanism for a wide variety of materials rendered under high-pressure conditions. Specifically, conformational changes, pressure-mediated hydrogen bonding interactions, molecular and crystal structural transitions, polymerizations and photon-assisted chemical reactions, as well as guest-host interactions of respective selected systems can be efficiently and accurately probed and characterized using *in situ* high-pressure Raman spectroscopy, FTIR spectroscopy or combination of both. These spectroscopic data provided enormously valuable information for us to understand the pressure-induced phenomena at microscopic level in-depth. Thus, vibrational micro-spectroscopy can be considered a routine but indispensable technique in any high-pressure materials research laboratories.

In addition to extreme pressure, extreme temperatures such as several Kelvin and several hundred degrees Celsius, and especially their combinations pose experimental challenges yet offer new and unexplored P-T domains for novel structures and properties of materials to be discovered. *In situ* vibrational micro-spectroscopy is expected to play an important role in structural characterization under these tough conditions. Although extremely convenient, one should realize that vibrational spectroscopy itself alone is seldom successful in solving totally unknown structures. Therefore, to realize the full potential of vibrational spectroscopy on materials under extreme conditions, other experimental techniques such as X-ray diffraction, synchrotron probes as well as theoretical modeling are essential to obtain the full structural information of novel materials.

Acknowledgements

This work was supported by a Discovery Grant, a Research Tools and Instruments Grant from the Natural Science and Engineering Research Council of Canada, a Leaders Opportunity Fund from the Canadian Foundation for Innovation, an Early Researcher Award from the Ontario Ministry of Research and Innovation, a Petro-Canada Young Innovator Award and by Defense Research and Development Canada under contract No. W7702-135601. The synchrotron IR measurements presented were performed at U2A beamline of National Synchrotron Light Source of US Brookhaven National Laboratory.

Author details

Yang Song

Address all correspondence to: yang.song@uwo.ca

Department of Chemistry, University of Western Ontario, London, Ontario, Canada

References

[1] Song Y, Manaa MR. New trends in chemistry and materials science in extremely tight space. J Phys Chem C. 2012;116:2059–60.

[2] Hemley RJ, Ashcroft NW. The revealing role of pressure in the condensed matter sciences. Phys Today. 1998;51:26–32.

[3] Hemley RJ. Effects of high pressure on molecules. Annu Rev Phys Chem. 2000;51:763–800.

[4] Schettino V, Bini R. Molecules under extreme conditions: Chemical reactions at high pressure. Phys Chem Chem Phys. 2003;5:1951–65.

[5] McMillan PF. Chemistry at high pressure. Chem Soc Rev. 2006;35:855–7.

[6] Grochala W, Hoffmann R, Feng J, Ashcroft NW. The chemical imagination at work in very tight places. Angew Chem-Int Edit. 2007;46:3620–42.

[7] Schettino V, Bini R. Constraining molecules at the closest approach: chemistry at high pressure. Chem Soc Rev. 2007;36:869–80.

[8] Song Y. New perspectives on potential hydrogen storage materials using high pressure. Phys Chem Chem Phys. 2013;15:14524–47.

[9] Mao HK, Bell PM, Shaner JW, Steinberg DJ. Specific volume measurements of copper, molybdenum, palladium, and silver and calibration of the ruby R1 fluorescence pressure gauge from 0.06 to 1 mbar. J Appl Phys. 1978;49:3276–83.

[10] Dong Z. High-pressure study of molecular solids and 1D nanostructures by vibrational spectroscopy and synchrotron X-ray diffraction [Thesis]: University of Western Ontario; 2012.

[11] Dong Z, Song Y. Transformations of cold-compressed multiwalled boron nitride nanotubes probed by infrared spectroscopy. J Phys Chem C. 2010;114:1782–8.

[12] Sabharwal RJ, Huang Y, Song Y. High-pressure induced conformational and phase transformations of 1,2-dichloroethane probed by Raman spectroscopy. J Phys Chem B. 2007;111:7267–73.

[13] Dong Z, Beilby NG, Huang Y, Song Y. Conformational and phase transformations of chlorocyclohexane at high pressures by Raman spectroscopy. J Chem Phys. 2008;128:074501.

[14] Murli C, Lu N, Dong Z, Song Y. Hydrogen bonds and conformations in ethylene glycol under pressure. J Phys Chem B. 2012;116:12574–80.

[15] Zhou L, Shinde N, Hu A, Cook C, Murugesu M, Song Y. Structural tuning of energetic material Bis(1H-tetrazol-5-yl)amine monohydrate under pressures probed by vibrational spectroscopy and X-ray diffraction. J Phys Chem C. 2014;118:26504–12.

[16] Dong Z, Seemann NM, Lu N, Song Y. Effects of high pressure on azobenzene and hydrazobenzene probed by Raman spectroscopy. J Phys Chem B. 2011;115:14912–8.

[17] Zhuravlev KK, Traikov K, Dong Z, Xie S, Song Y, Liu Z. Raman and infrared spectroscopy of pyridine under high pressure. Phys Rev B. 2010;82:064116.

[18] Xie S, Song Y, Liu Z. In situ high-pressure study of ammonia borane by Raman and IR spectroscopy. Can J Chem. 2009;87:1235–47.

[19] Liu A, Xie S, Dabiran-Zohoory S, Song Y. High-pressure structures and transformations of calcium borohydride probed by combined Raman and infrared spectroscopies. J Phys Chem C. 2010;114:11635–42.

[20] Liu A, Song Y. In situ high-pressure study of sodium amide by Raman and infrared spectroscopies. J Phys Chem B. 2011;115:7–13.

[21] Liu A, Song Y. In situ high-pressure and low-temperature study of ammonia borane by Raman spectroscopy. J Phys Chem C. 2012;116:2123–31.

[22] Chen JH, Couvy H, Liu HZ, Drozd V, Daemen LL, Zhao YS, et al. In situ X-ray study of ammonia borane at high pressures. Int J Hydrogen Energy. 2010;35:11064–70.

[23] Murli C, Song Y. Pressure-induced polymerization of acrylic acid: a Raman spectroscopic study. J Phys Chem B. 2010;114:9744–50.

[24] Guan J, Song Y. Pressure selected reactivity and kinetics deduced from photoinduced dissociation of ethylene glycol. J Phys Chem B. 2015;119:3535–45.

[25] Hu Y, Kazemian H, Rohani S, Huang Y, Song Y. In situ high pressure study of ZIF-8 by FTIR spectroscopy. Chem Commun. 2011;47:12694–6.

[26] Hu Y, Liu Z, Xu J, Huang Y, Song Y. Evidence of pressure enhanced CO_2 storage in ZIF-8 probed by FTIR Spectroscopy. JACS. 2013;135:9287–90.

[27] Hu Y, Lin B, He P, Li Y, Huang Y, Song Y. The structural stability of and enhanced CO_2 storage in MOF MIL-68 (In) under high pressures probed by FTIR spectroscopy. Chem Eur J. 2015;21:18739–48.

IntechOpen